

Design and fabrication of a time-of-flight spectrometer for studies of multiple ionization of gases by charged particle impact

R K SINGH, R K MOHANTA, M J SINGH¹, R HIPPLER², S K GOEL³ and R SHANKER

Atomic Physics Laboratory, Physics Department, Banaras Hindu University, Varanasi 221 005, India

¹Institute for Plasma Research, Near Indira Bridge, Bhat, Gandhinagar 382 428, India

²Fachbereich Physik, Universitaet Greifswald, Domstrasse 10a, 17487 – Greifswald, Germany

³Technology Information, Forecasting and Assessment Council (TIFAC), DST, New Delhi 110 016, India

Email: rshanker@banaras.ernet.in

MS received 26 March 2001; revised 18 October 2001

Abstract. A time-of-flight spectrometer has been designed and fabricated for measuring the charge state distributions of target ions produced in collisions of keV-electrons with gaseous target atoms/molecules. The design details of the spectrometer and the description of experimental procedures for optimizing various parameters are presented and discussed. The working principle of the spectrometer, its time- and mass-focussing conditions, transmissions and detection efficiency etc. are given. A few typical test runs on multiple ionization of Ne and Ar gas atoms are illustrated. These spectra are found to yield the time resolution of about 10 ns for Ar⁴⁺ ion peak in 24.0 keV e⁻ – Ar collisions while the mass resolution of the spectrometer is obtained about 10% at mass $m = 20$.

Keywords. Recoil ions; time-of-flight (TOF) spectrometer; multiple ionization.

PACS Nos 29.25.-t; 34.70.+e

1. General considerations

The time-of-flight spectrometer in its simplest form, consists of an ion source and an ion-collector fixed at two opposite ends of an evacuated tube. The ions formed in the ion source, for example, in electron–atom/molecule collisions are extracted out and are made to move towards the collector under a constant or a pulsed electric field. In either case, the time-of-flight of the ions is proportional to $\sqrt{(m/q)}$ where q is the charge state and m is the mass of ions.

A time-of-flight spectrometer possesses the following salient features:

- (i) speed of collection of ions at the collector is relatively fast ($< 1 \mu s$),

- (ii) if a pulsed accelerating field is used, then for each accelerating pulse, the entire spectrum is recorded in one pulse event. Thus, it is possible to measure the relative intensities accurately, even though source conditions may vary rapidly,
- (iii) extremely accurate mechanical alignment of TOF spectrometer is not required. Also, for doing accurate measurements, production of highly uniform stable magnetic fields is not required. Thus freedom from stringent geometric conditions simplifies construction and dispensing with magnetic field removes shape and size restrictions.

2. Theoretical considerations

In this paper, we have taken the theoretical treatment on the time-of-flight spectrometer from a paper cited in ref. [1]. Ideally, if all the ions are formed parallel to the source electrodes, that is, along the axis of TOF spectrometer and with zero initial velocity of the ion, then the flight-times of all the ions having identical m/q will be the same. For such a case, the resolution is limited solely by the resolution of the ion-detecting device. But this is not always the case. Generally there is a 'time-spread' caused by the initial spatial and kinetic energy or velocity distributions of ions. Thus, it can be said that the width of time resolution of the TOF spectrometer is governed by width of the spatial and the velocity distributions and they add in quadrature to give the total time resolution. Hence, to obtain a good time resolution, the width due to these two distributions should be minimized.

Therefore, the overall time-resolution of a TOF spectrometer can be written as the resultant of

- space distribution and
- time spread due to energy distribution of ions in the ion source.

2.1(a) *Time spread due to space distribution:* The space distribution is considered to be the deviation Δs of the initial position of birth of the ion in a given charge state about its average position s_0 . It can assume a maximum and a minimum value such that

$$s_{\max} = s_0 + \frac{1}{2}\Delta s \quad \text{and} \quad s_{\min} = s_0 - \frac{1}{2}\Delta s.$$

One may consider the space distribution to originate from two basic sources:

- (i) a finite beam width and
- (ii) a spread of the gas target atoms about s_0 .

Time spread $\Delta T_{\Delta s}$ due to space distribution can be reduced in two ways:

- (i) by making Δs as small as possible,
- (ii) by space focusing, which gives each ion a velocity dependence on s in such a way as to minimize $\Delta T_{\Delta s}$.

2.1(b) *Time spread due to initial velocity distribution:* The time spread is caused by randomly directed velocities of the ions. The maximum time spread is, therefore given by identical ions formed at the same position but with oppositely directed velocities.

The time spread can be reduced in two ways by:

- (i) increasing the ratio of ion's total energy (E) to its initial energy (E_0) by varying voltages in different accelerating regions, i.e. $E/E_0 \gg 1$
- (ii) introducing a time lag between the creation of ions and their accelerations.

2.2 Mass resolution

The maximum resolvable mass [1] depends on the initial space and energy distribution functions. Consider the relation

$$1/m = 1/m_s + 1/m_\theta \quad (1)$$

where m_s and m_θ are the maximum resolvable masses for which time spread due to space distribution of ions ΔT_s equals the time spread between adjacent mass peaks and time spread due to kinetic energy distribution of ions ΔT_θ equals the time between adjacent mass peaks respectively. m will take smaller values than either m_s or m_θ . On the other hand, it will be at least as large as the value m obtained above by assuming the total spread to be the sum of the energy and the space time spreads.

2.3 Choice of accelerating region

Wiley and McLaren [1] have compared the TOF spectrometers with a single accelerating and a double accelerating regions.

For a TOF spectrometer having a single accelerating region, $E_d = 0$ and $d = 0$ where E_d is the electric field in second accelerating region (see figure 1).

The advantage of having a second accelerating region is that it has two parameters, d and E_d to play with. This flexibility makes the double field source easier to adjust, thereby yielding a better resolution.

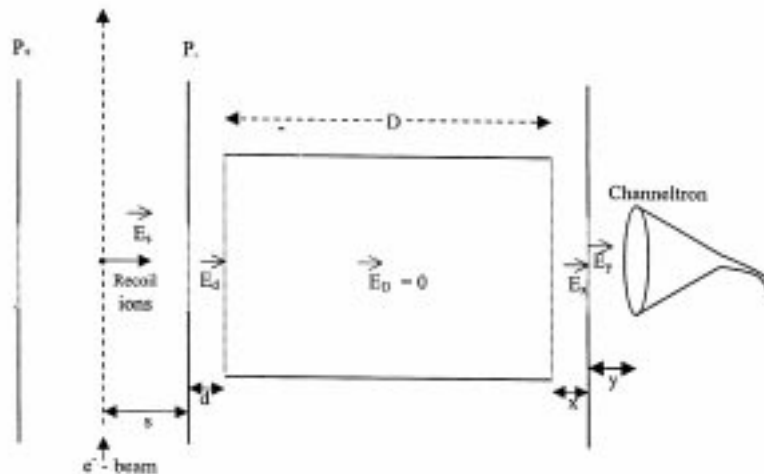


Figure 1. Working principle diagram of a time-of-flight spectrometer. For explanations of the symbols, see the text.

2.4 Total energy and time-of-flight of ions with two accelerating regions

2.4.1 Total energy: During its flight towards the collector (see figure 1), any ion born with energy U_0 will increase its energy to U depending on

- (i) s
- (ii) U_0 and
- (iii) Charge state q .

Therefore, the total energy U of the ion reaching the collector is given by

$$U = U_0 + qsE_s + qdE_d \quad (2)$$

where E_s is the electric field in the first accelerating region and E_d the electric field in the second accelerating region.

2.4.2 Time of flight: The total time T taken by an ion in a particular charge state q and a mass m in reaching the collector is given by

$$T(U_0, s) = T_s + T_d + T_D \quad (3)$$

where T_s is the flight time in the first accelerating region, T_d the flight time in the second accelerating region and T_D the flight time in the drift tube.

$$T_s = \left[\frac{(2m)^{1/2}}{qE_s} \right] [(U_0 + qsE_s)^{1/2} \pm U_0^{1/2}]. \quad (4a)$$

The (+) and (-) signs correspond to the initial velocity of the ion directed respectively away from and toward the collector.

$$T_d = \left[\frac{(2m)^{1/2}}{qE_d} \right] [(U_0 + qsE_s + qdE_d)^{1/2} (U_0 + qsE_s)^{1/2}]$$

or

$$T_d = \left[\frac{(2m)^{1/2}}{qE_d} \right] [U^{1/2} - (U_0 + qsE_s)^{1/2}] \quad (4b)$$

$$T_D = \frac{(2m)^{1/2}D}{2U^{1/2}} \quad (4c)$$

where D is the length of the drift tube.

It should be noted that s represents the distance of the first extractor plate from the point where ion is born. Because of finite width of beam and gas target

$$s = s_0 \pm \frac{1}{2} \Delta s.$$

Suppose $U_0 = 0$ and $s = s_0$. Then

$$U = qs_0E_s + qdE_d.$$

Then, the TOF T of an ion in a charge state q and a mass m is given by

$$T(0, s_0) = \frac{(2m)^{1/2}}{q} \left[\frac{a^{1/2}}{E_s} + \frac{b^{1/2} - a^{1/2}}{E_d} + \frac{qD}{2b^{1/2}} \right] \quad (5)$$

where $a = qs_0E_s$ and $b = qs_0E_s + qdE_d$.

2.4.3 *Space resolution*: Space focussing depends on the fact that an ion initially closer to the detector acquires less energy and is therefore eventually overtaken by ions which have large initial s values. To find the position at which ions whose initial values were $s = s_0 \pm \frac{1}{2}\Delta s$ pass each other, set $(dT/ds)_{U_0, s_0} = 0$. Using eq. (5), one obtains the expression for the length of the drift tube D as,

$$D = 2(s_0E_s + dE_d)^{3/2} \left[\frac{1}{(s_0E_s)^{1/2}} \left(\frac{1}{E_s} - \frac{1}{E_d} \right) + \frac{1}{(s_0E_s + dE_d)^{1/2}} \frac{1}{E_d} \right]. \quad (6)$$

Thus, for a single value of s_0 , E_s , d and E_d one can find out an optimum value of D for which the time spread due to initial space distribution is almost negligible. Equation (6) is the condition for space focusing for a double field system.

For a single field system $d = 0$, $E_d = 0$. Therefore, from eq. (6), one obtains the condition $D = 2s_0$ for optimum space focusing.

2.5 Time spread due to initial energy distribution

Identical ions born at the same place can have their initial velocities directed either away from the collector or towards it. An ion-1 initially having a velocity directed away from the collector will be decelerated by the field E_s until it comes to rest and then it starts its motion towards the collector, i.e. in the direction of the field E_s . Thus, comparing the ion born at the same place but with a velocity directed towards the collector, the ion-1 lags behind the ion-2 by the 'turn around time'. Thus, the time spread (ΔT_θ) due to initial energies is nothing but the 'turn around time' and it is given by

$$\Delta T_\theta = \text{Turn around time} = 2 \text{ deceleration time} = \frac{2(2mU_0)^{1/2}}{qE_s}. \quad (7)$$

2.6 Time of flight arrangement for studying the charge state distribution of ions in the present setup

If the ions are born with an initial energy U_0 , then the total energy U of the ions in the charge state q impinging on the detector (see figure 1) is given by

$$U = U_0 + qsE_s + qdE_d + qxE_x + qyE_y. \quad (8)$$

The total time of flight of the ion from its point of birth to the detector is

$$T = T_s + T_d + T_D + T_x + T_y, \quad (9)$$

$$T_s = \frac{(2m)^{1/2}}{qE_s} [(U_0 + qsE_s)^{1/2} - U_0^{1/2}], \quad (10a)$$

$$T_d = \frac{(2m)^{1/2}}{qE_d} [(U_0 + qsE_s + qdE_d)^{1/2} - (U_0 + qsE_s)^{1/2}], \quad (10b)$$

$$T_D = \frac{(2m)^{1/2}D}{2(U_0 + qsE_s + qdE_d)^{1/2}}, \quad (10c)$$

$$T_x = \frac{(2m)^{1/2}}{qE_x} [(U_0 + qsE_s + qdE_d + qxE_x)^{1/2} - (U_0 + qsE_s + qdE_d)^{1/2}], \quad (10d)$$

$$T_y = \frac{(2m)^{1/2}}{qE_y} [(U_0 + qsE_s + qdE_d + qxE_x + qyE_y)^{1/2} - (U_0 + qsE_s + qdE_d + qxE_x)^{1/2}]. \quad (10e)$$

Substituting values of T_s , T_d , T_D , T_x and T_y in eq. (9) and assuming that the ion is born with initial velocity $U_0 = 0$, the time of flight is given by the equation

$$T = \frac{(2m)^{1/2}}{q} \left[\frac{a^{1/2}}{E_s} + \frac{b^{1/2} - a^{1/2}}{E_d} + \frac{qD}{2b^{1/2}} + \frac{c^{1/2} - b^{1/2}}{E_x} + \frac{d^{1/2} - c^{1/2}}{E_y} \right] \quad (11)$$

where $a = qsE_s$, $b = qsE_s + qdE_d$, $c = qsE_s + qdE_d + qxE_x$ and $d = qsE_s + qdE_d + qxE_x + qyE_y$.

For optimum space resolution, as discussed earlier, putting $(dT/ds) = 0$, it gives the drift length

$$D = 2(sE_s + dE_d)^{3/2} \left[\frac{1}{(sE_s)^{1/2}} \left\{ \frac{1}{E_s} - \frac{1}{E_d} \right\} + \frac{1}{(sE_s + dE_d)^{1/2}} \times \left\{ \frac{1}{E_d} - \frac{1}{E_x} \right\} + \frac{1}{(sE_s + dE_d + xE_x)^{1/2}} \left\{ \frac{1}{E_x} - \frac{1}{E_y} \right\} + \left\{ \frac{1}{sE_s + dE_d + xE_x + yE_y} \right\}^{1/2} \frac{1}{E_y} \right]. \quad (12)$$

Parameters chosen for the present TOF are displayed in table 1.

Using the data from table 1 in eq. (12), we find the value of $D = 2.3 \pm 0.1$ cm.

Table 1. Experimentally optimized parameters of the TOF spectrometer.

Distance of the interaction point from P_- s	9 mm
Distance of the drift tube from P_- d	3 mm
Length of the drift tube D	22 mm
Distance of post acceleration plate from the drift tube x	3 mm
Distance of channeltron from the post acceleration plate y	5 mm
Voltage on P_+	190 V
Voltage on P_-	-190 V
Voltage on drift tube	-215 V
Voltage on post acceleration plate	-800 V
Voltage on channeltron	-2950 V

3. Design and fabrication of the TOF spectrometer

A schematic diagram of the TOF set-up is shown in figure 2. It has an interaction zone enclosed between two electrodes, P_+ and P_- , where the electron beam crosses a beam of neutral gaseous atoms effusing from a multicapillary tube or hypodermic needle. P_+ is the SS-grid (transparency 80%) of circular form of diameter 10 mm through which the ejected electrons pass through. P_- is the SS-circular disc of diameter 10 mm. The separation between P_+ and P_- is 18 mm. A positive voltage on the P_+ and an equal negative voltage on the P_- help in pulling out the electrons and ions respectively from their birthplaces in the opposite directions. A 3 mm hole in P_- electrode provides a passage for the ions to come out from the interaction zone. The hole is covered with a SS-grid of parallel wires having 80% transmission efficiency for maintaining the uniform electric field. Once out of the hole, the ions are accelerated over a distance d (3 mm) before they enter an aluminium drift tube D of length 22 mm and diameter 10 mm. After coming out from the drift tube, ions are accelerated over a distance x (3 mm) and pass through a 3 mm hole of the last accelerating plate A. The accelerating plate A is a SS-disc of 10 mm diameter with 3 mm hole on it; it is kept at -800 V which provides the post acceleration for ions before impinge the cone of a channel electron multiplier (CEM). The cone voltage (E_y) is kept at about -2.95 kV and distance between last accelerating plate A and cone is $y = 5$ mm. The two ends of the drift tube and the hole of the plate A are again covered with grids of similar transmission as mentioned above. The assembly of plates, grids and drift tube is fixed on a series of teflon rings of diameter 24 mm. Teflon rings are aligned and supported by three SS-rods of 3 mm diameter. The rods are fixed in the teflon rings at 120° from each other.

4. Experimental tests and optimization of the TOF spectrometer

Test measurements [2] were carried out to determine the charge state fractions of the target ions. The properties of the TOF spectrometer and the functioning of its various components are checked and discussed in the following subsections.

4.1 Complete extraction of ions from a defined collision region

The collision region is the volume in front of the extraction hole in negative electrode P_- of the condenser (see figure 2). The extraction of recoil ions in a singly charged state

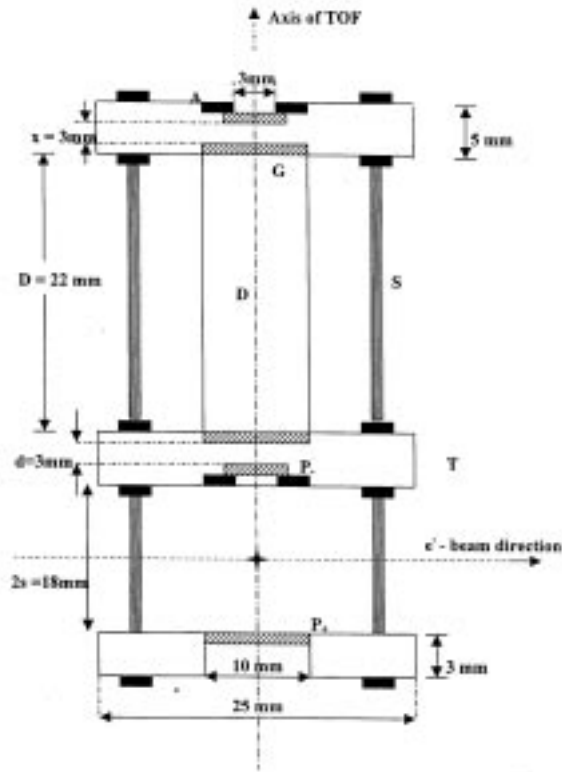


Figure 2. Schematic diagram of TOF spectrometer: P_+ and P_- – extracting plates; D – drift tube; A – post accelerating plate.

was investigated by monitoring the normalized number of these ions to the total charge of incident electrons collected at a biased Faraday cup (-60 V) as a function of the extraction voltage. At low electric field strengths, the ion count rate increases with the voltage; however, for fields greater than about 160 V/cm, the recoil ion count rate is found to become constant (see figure 3) indicating a condition for ‘complete extraction’ of the ions. This condition was achieved when the post acceleration voltage was kept at -800 V while the CEM mouth-voltage was maintained at -2950 V.

4.2 Equal transmission for all recoil ions

The drift tube length D was chosen to be 2.2 cm in our TOF spectrometer. This length gives the best timing resolution in the test runs. This has been confirmed also by calculating the drift tube length using eq. (12) with our optimized experimental parameters. The calculated value of D is found to be 2.3 ± 0.1 cm. Also, we have calculated the total flight times of Ar-ions in different charge states including the time spread due to initial

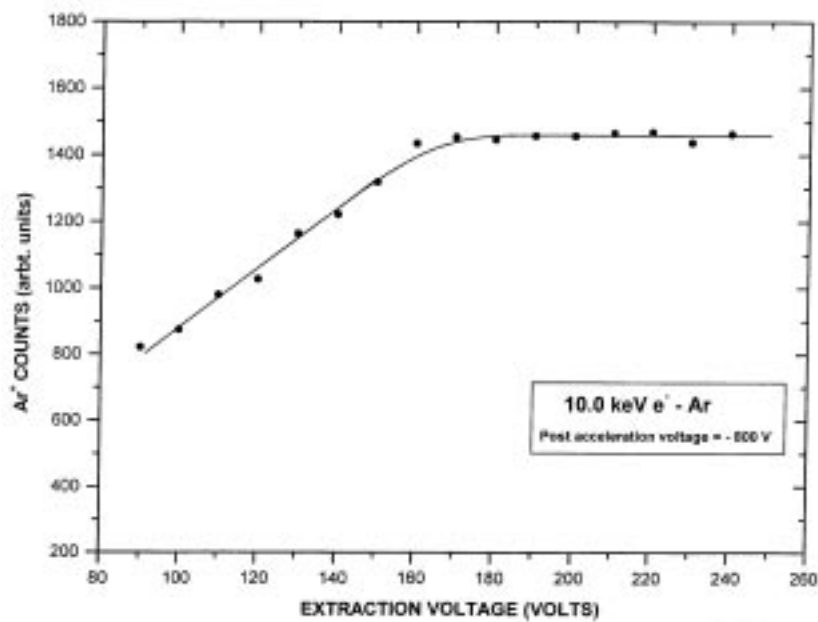


Figure 3. Variation of beam normalized Ar^+ ion counts as a function of ion extracting voltage at a drift tube voltage of -215 V.

space distribution for an optimum drift tube length (see table 2). These calculations have been used to plot a graph between the time-of-flight (ns) and a range of space spread Δs (mm) values at $D = 2.2$ cm for $1+$, $2+$, $3+$ and $4+$ argon ions (see figure 4). From the graph, it is seen that the time spread due to initial space distribution is negligible for $\Delta s = |0.2|$ cm. Further calculations have been made to see the effect of variation in drift tube length D on the space focusing due to initial space distribution of argon ions. The results are contained in table 3 and the corresponding graphs are shown in figures 5a and 5b. From these graphs, it is noted that there is an appreciable amount of time spread due to initial space distribution if the drift tube length D is kept less than or greater than the optimum drift length of 2.2 cm by, for example, ± 0.5 cm.

4.3 Equal detection probability for all recoil ions

It has been shown earlier [3] that above a certain detection voltage applied to CEM, the detection probability is independent of the ion energy and the point of impact on the CEM. This was ensured by studying the variation of bias voltage applied on the mouth of CEM detector as a function of Ar^+ counts (see figure 6). It is observed that as the CEM bias voltage is increased, the ion counts also increase steadily, however, at bias voltages larger than -2.8 kV, the ion count rates tend to become constant. This feature indicates that even the slowest ion, that is Ar^+ , is able to reach the detector with equal efficiency along with the other higher charged state ions. Thus, this test ensures the condition for equal detection probability for all recoil ions.

Table 2. Data showing the effect of initial space distributions on time-of-flight (ns) of argon ions in different charge states at optimum drift tube length $D = 2.2$ cm.

Charge state q	$S = 0.70$ $\Delta s = -0.2$	$S = 0.75$ $\Delta s = -0.15$	$S = 0.80$ $\Delta s = -0.1$	$S = 0.85$ $\Delta s = -0.05$	$S = 0.9$ $\Delta s = 0$	$S = 0.95$ $\Delta s = 0.05$	$S = 1.0$ $\Delta s = +0.1$	$S = 1.05$ $\Delta s = 0.15$	$S = 1.1$ $\Delta s = +0.2$	$S = 1.15$ $\Delta s = 0.25$
1	1526.5	1524.0	1523.4	1523.7	1523.2	1523.7	1525.1	1527.3	1529.7	1532.7
2	1079.4	1077.6	1077.2	1077.4	1077.1	1077.4	1078.4	1080.0	1081.7	1083.8
3	881.3	879.9	879.5	879.7	879.4	879.7	880.5	881.8	883.2	884.9
4	763.3	762.0	761.7	761.9	761.6	761.9	762.6	763.7	764.9	766.4

Table 3. Calculations showing the effect of initial space distributions on time-of-flight (ns) of argon ions in different charge states for two drift lengths.

Charge state q	$S = 0.70$ $\Delta s = -0.2$	$S = 0.75$ $\Delta s = -0.15$	$S = 0.80$ $\Delta s = -0.1$	$S = 0.85$ $\Delta s = -0.05$	$S = 0.9$ $\Delta s = 0$	$S = 0.95$ $\Delta s = 0.05$	$S = 1.0$ $\Delta s = +0.1$	$S = 1.05$ $\Delta s = 0.15$	$S = 1.1$ $\Delta s = +0.2$	$S = 1.15$ $\Delta s = 0.25$
$D = 1.7$ ($\Delta D = -0.5$)										
1	1363.7	1365.7	1368.6	1371.4	1374.1	1378.4	1382.3	1386.6	1391.7	1396.7
2	964.3	965.7	967.7	969.7	971.6	974.7	977.4	980.5	984.1	987.6
3	787.3	788.5	790.2	791.8	793.3	795.8	798.1	800.6	803.5	806.4
4	681.9	682.9	684.3	685.7	687.1	689.2	691.2	693.3	695.9	698.4
$D = 2.7$ ($\Delta D = +0.5$)										
1	1688.8	1683.3	1679.2	1675.4	1671.9	1670.4	1668.8	1667.9	1668.0	1668.4
2	1194.2	1190.3	1187.4	1184.7	1182.2	1181.2	1180.0	1179.4	1179.5	1179.7
3	975.0	971.9	969.5	967.3	965.3	964.4	963.5	963.0	963.0	963.2
4	844.4	841.7	839.6	837.7	836.0	835.2	834.4	834.0	834.0	834.2

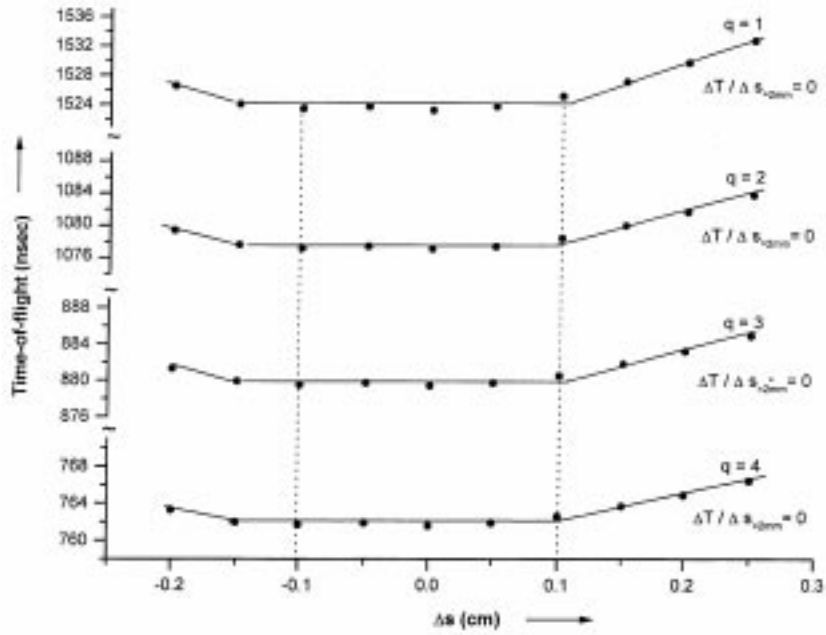


Figure 4. Graph plotted between the calculated time-of-flight (ns) of different charge states q of argon ions as a function of initial space distribution Δs at an optimum drift tube length, $D = 2.2$ cm (see eq. (11)).

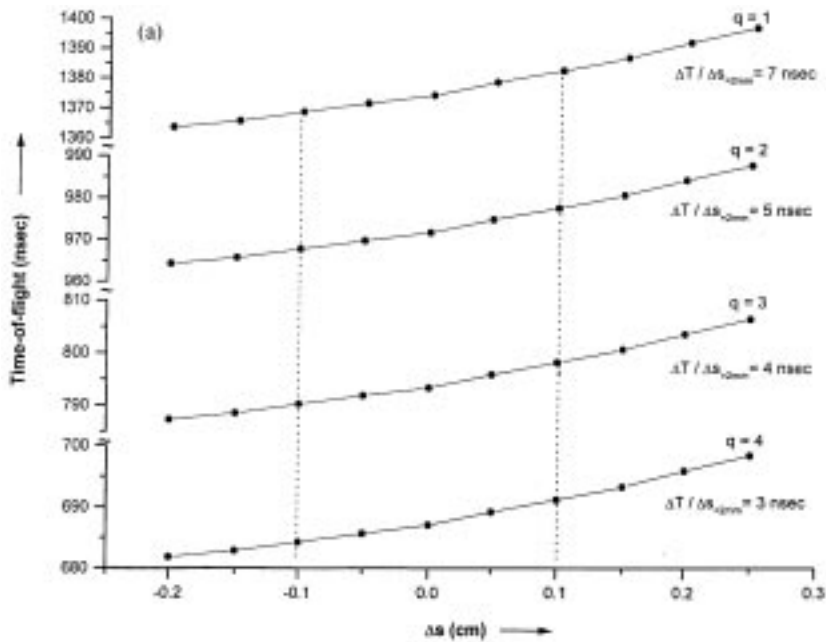


Figure 5a.

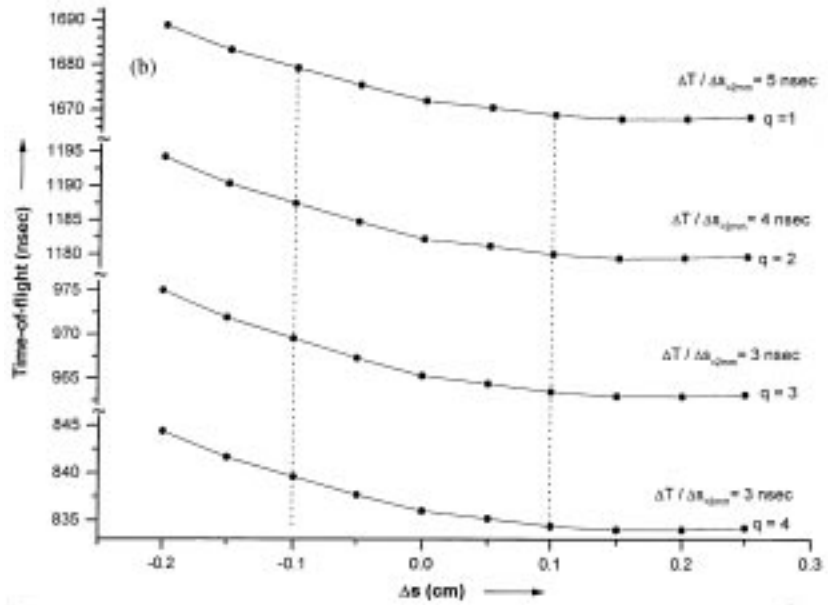


Figure 5. (a) Graph plotted between the calculated time-of-flight (ns) of different charge states q of argon ions as a function of initial space distribution Δs for $D = 1.7$ ($\Delta D = -0.5$ cm). (b) Graph plotted between the calculated time-of-flight (ns) of different charge states q of argon ions as a function of initial space distribution Δs for $D = 2.7$ ($\Delta D = +0.5$ cm).

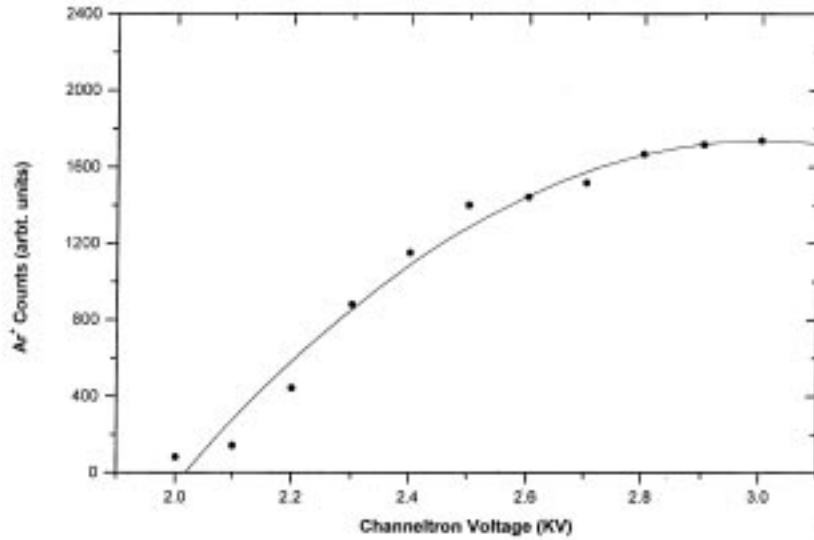


Figure 6. Variation of beam normalized Ar⁺ ion counts as a function of cone voltage of the channel electron multiplier (CEM).

4.4 Single collision condition

The single collision condition is an essential and important step to establish while measuring the cross sections of a particular collision reaction. It is because the recoil ions during their transit from the birth place to the detector may undergo further collisions which could change their initial charge states. This requirement is satisfied by doing measurements at different target gas pressures. Over a wide range of pressures, the count rate of an ion say, Ar^+ is found to be proportional to the pressure. Further, the multiple collision events are clearly seen to set in at pressures beyond 5×10^{-4} torr. The operating pressure for a single collision condition in the present experiments is thus taken to be 2.4×10^{-4} torr (see figure 7).

5. Ion detection and charge state analysis

The collision induced ions are detected by a CEM in the pulse counting mode. The CEM was purchased from M/s Dr. Sjuts GmbH, Germany. It is coupled to a preamplifier (ORTEC, model VT-120, gain 200) via a 1000 pF high voltage capacitor. The CEM and the preamplifier are enclosed in an aluminium case. The output signal from the CEM is attached with the preamplifier by a short 50 Ω coaxial cable. The charge state analysis of the ions that are produced in the collision zone is made on the basis of their respective time-of-flight to the detector.

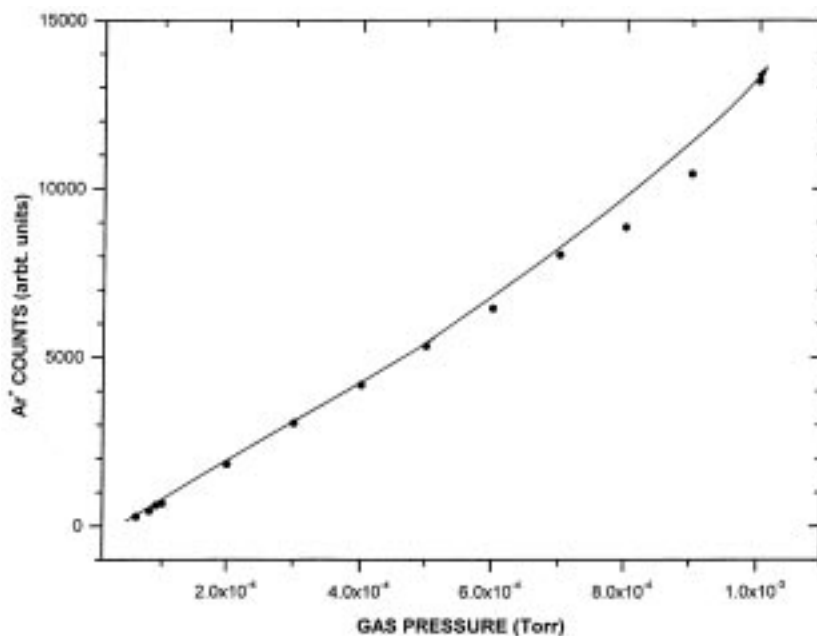


Figure 7. Change of argon gas pressure as a function of beam normalized Ar^+ ion counts. 'A single collision condition' is seen to set in for pressures less than 5.0×10^{-4} torr.

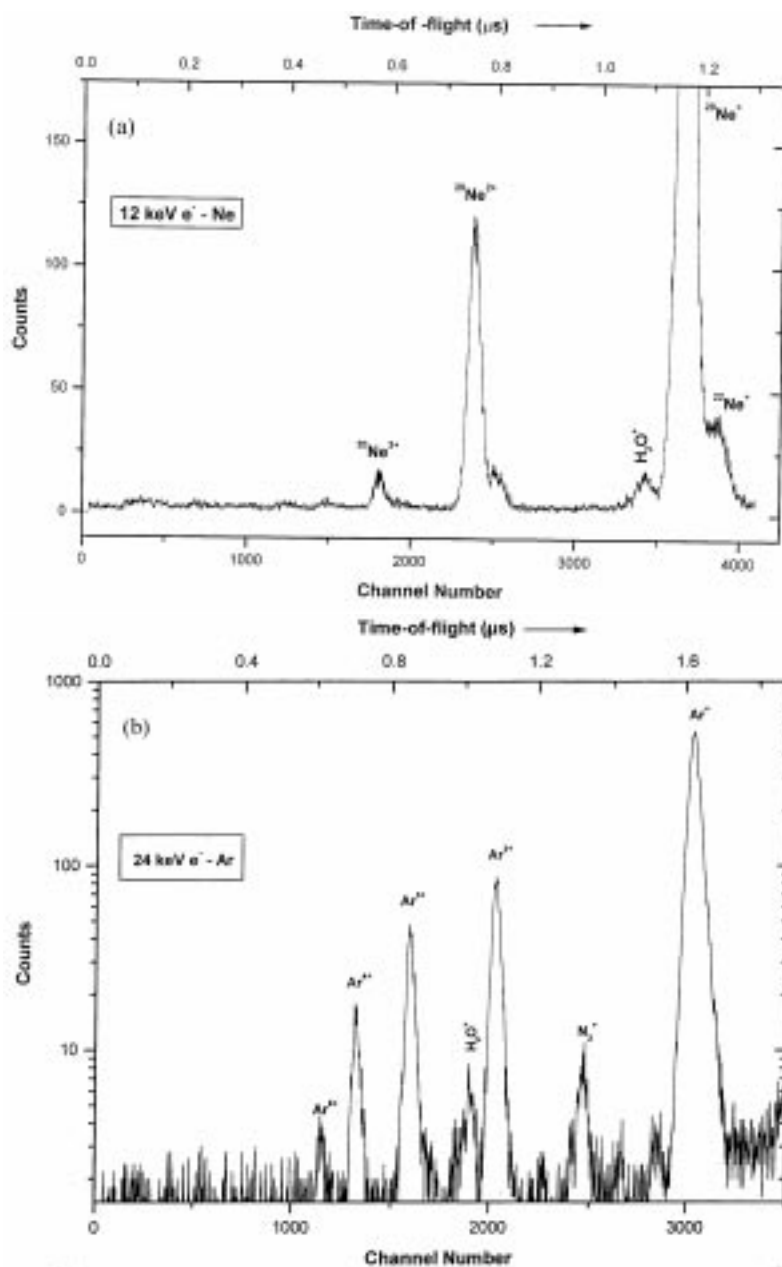


Figure 8. (a) A typical time-of-flight spectrum of Ne^{n+} ions ($n = 1-3$) produced in 12.0 keV e^- -Ne collisions. Spectra are recorded by observing the coincidences between neon ions and simultaneously ejected electrons of all energies at 90° with respect to incident beam in a single collision condition. (b) Time-of-flight spectrum of Ar^{n+} ions ($n = 1-5$) produced in 24.0 keV e^- -Ar collisions. The spectra are obtained by following the same procedure as stated in figure 8a.

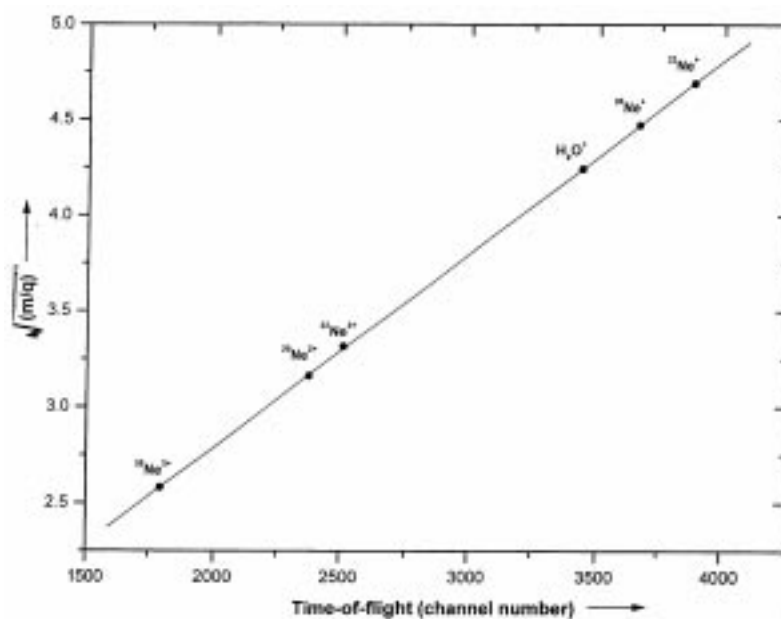


Figure 9. A calibration curve for identifying different peaks in the time-of-flight spectra is plotted between $\sqrt{(m/q)}$ and time-of-flight (or channel number).

In order to measure the time-of-flight spectrum of ions, we employ a standard fast/slow coincidence circuit. The ion pulses are used as STOP and the simultaneously ejected electrons from the collision zone serve as START pulse to a time-to-amplitude converter (TAC). A detailed description of the experimental procedures for measuring the time spectra is given in ref. [4].

6. Test spectra employing the TOF spectrometer

We have measured the time-of-flight spectra of multiply charged neon and argon ions produced in 12.0 keV e^- -Ne and 24.0 keV e^- -Ar collisions using our TOF spectrometer in coincidence with the ejected electrons of all energies at 90° to the incident electron beam direction. The electrons are detected by another CEM (M/s Amptek Inc. USA, model MD-501) in the pulse counting mode. Ne^{n+} and Ar^{n+} ions with charge states n up to 3+ and 5+ respectively are clearly seen in the spectrum (see figures 8a and 8b). A few ion peaks originating from residual gases, for instance, H_2O^+ and N_2^+ are also identified in addition to the neon and argon ion peaks. The multiply charged argon ion peaks are well separated in time and give a typical time resolution of about 10 ns for Ar^{4+} peak in 24.0 keV e^- -Ar collisions. Also the ^{20}Ne and ^{22}Ne isotopic ion peaks produced in 12.0 keV e^- -Ne collisions are seen to be separated by a reasonably good time difference (70 ns). Thus, the mass resolution of the spectrometer can be stated to be about 10% at $m = 20$. A calibration curve to identify different ion peaks in the time-of-flight spectrum has been obtained by plotting a graph between $\sqrt{(m/q)}$ and the time-of-flight (or channel number); see figure 9. This

performance of the TOF spectrometer is found to be satisfactory. Undoubtedly, it gives us confidence to employ its suitability for measuring different charge states or mass numbers of ions under investigation as the case may be.

7. Conclusions

A TOF spectrometer has been designed and fabricated indigenously. It has been fully optimized for its performance with regard to extraction, transmission and detection efficiencies for recoil ions in different charge states. The performance of the present TOF spectrometer has been tested by recording the charge state distributions of neon and argon multiply charged ions produced in collisions of 12.0 keV and 24.0 keV electrons with neon and argon gases respectively in a single collision condition. The charge states up to 3+ in neon and 5+ in argon have been observed. The ^{20}Ne and ^{22}Ne isotopic ions are also seen clearly separated. The typical values of time resolution and that of mass resolution are found to be respectively about 10 ns for Ar^{4+} ions produced in 24.0 keV e^- -Ar collisions and about 10% at mass $m = 20$. Thus, the overall performance of the spectrometer is found to be satisfactory. This spectrometer is to be used in studies related to the collision dynamics of recoil ions produced in keV electron-atom/molecule collisions.

Acknowledgment

The financial support extended by the Department of Science and Technology (DST), New Delhi, India and the Deutsche Forschungsgemeinschaft (DFG), Germany are gratefully acknowledged for executing the developmental work. R K Singh and R K Mohanta are thankful to receive the fellowships from DST during the tenure of the research project.

References

- [1] W C Wiley and I H McLaren, *Rev. Sci. Instrum.* **26**, 1150 (1955)
- [2] W Groh, A Muller, A S Schlachter and E Salzbom, *J. Phys.* **B16**, 1997 (1983)
- [3] J Fricke, A Muller and E Salzbom, *NIM* **175**, 379 (1980)
- [4] R K Singh, R K Mohanta, R Hippler and R Shanker, *Pramana – J. Phys.* **58**, 1 (2002)